



Published in final edited form as:

*Thromb Haemost.* 2019 December ; 119(12): 1968–1980. doi:10.1055/s-0039-1697953.

## Urokinase Plasminogen Activator Overexpression Reverses Established Lung Fibrosis

Jeffrey C. Horowitz<sup>1</sup>, Daniel J. Tschumperlin<sup>2</sup>, Kevin K. Kim<sup>1</sup>, John J. Osterholzer<sup>1,3</sup>, Natalya Subbotina<sup>1</sup>, Iyabode O. Ajayi<sup>1</sup>, Seagal Teitz-Tennenbaum<sup>1,3</sup>, Ammara Virk<sup>1</sup>, Megan Dotson<sup>1</sup>, Fei Liu<sup>4</sup>, Delphine Sicard<sup>2</sup>, Shijing Jia<sup>1</sup>, Thomas H. Sisson<sup>1</sup>

<sup>1</sup>Division of Pulmonary and Critical Care Medicine, Department of Internal Medicine, University of Michigan, Ann Arbor, Michigan, United States

<sup>2</sup>Department of Physiology and Biomedical Engineering, Mayo Clinic, Rochester, Minnesota, United States

<sup>3</sup>Veterans Affairs Medical Center, Ann Arbor, Michigan, United States

<sup>4</sup>Department of Environmental Health, Harvard School of Public Health, Harvard University, Boston, Massachusetts, United States

### Abstract

**Introduction**—Impaired plasminogen activation (PA) is causally related to the development of lung fibrosis. Prior studies demonstrate that enhanced PA in the lung limits the severity of scarring following injury and in vitro studies indicate that PA promotes matrix degradation and fibroblast apoptosis. These findings led us to hypothesize that increased PA in an in vivo model would enhance the resolution of established lung fibrosis in conjunction with increased myofibroblast apoptosis.

**Methods**—Transgenic C57BL/6 mice with doxycycline inducible lung-specific urokinase plasminogen activator (uPA) expression or littermate controls were treated (day 0) with bleomycin or saline. Doxycycline was initiated on days 1, 9, 14, or 21. Lung fibrosis, stiffness, apoptosis, epithelial barrier integrity, and inflammation were assessed.

**Results**—Protection from fibrosis with uPA upregulation from day 1 through day 28 was associated with reduced parenchymal stiffness as determined by atomic force microscopy. Initiation of uPA expression beginning in the late inflammatory or the early fibrotic phase reduced stiffness and fibrosis at day 28. Induction of uPA activity in mice with established fibrosis decreased lung collagen and lung stiffness while increasing myofibroblast apoptosis. Upregulation of uPA did not alter lung inflammation but was associated with improved epithelial cell homeostasis.

**Conclusion**—Restoring intrapulmonary PA activity diminishes lung fibrogenesis and enhances the resolution of established lung fibrosis. This PA-mediated resolution is associated with

**Address for correspondence** Jeffrey C. Horowitz, MD, 6300 MSRB 3, 1150 West Medical Center Dr., Ann Arbor, MI 48109-5642, United States (jchorow@umich.edu).

Conflict of Interest

J.C.H., T.H.S., K.K.K., and D.J.T. report grants from National Institutes of Health, during the conduct of the study.

increased myofibroblast apoptosis and improved epithelial cell homeostasis. These studies support the potential capacity of the lung to resolve existing scar in murine models.

### Keywords

myofibroblast; apoptosis; plasminogen activators; wound healing; pulmonary fibrosis

---

### Introduction

Lung fibrosis is associated with an inhibition of plasminogen activator (PA) activity, and an increase in the expression of plasminogen activator inhibitor-1 (PAI-1) relative to the endogenous PAs (urokinase: uPA, and tissue: tPA) contributes to this inhibition in mouse models and in human disease.<sup>1</sup> Multiple studies have established a causal role for this imbalance between PAI-1 and the PAs in the development of lung fibrosis. For example, in studies from our laboratory, reconstituting PA activity via adenoviral-mediated overexpression of uPA on day 21 in bleomycin-injured mice resulted in decreased lung collagen content at day 28.<sup>2</sup> We also found that transgenic doxycycline-inducible upregulation of uPA expression in type II alveolar epithelial cells beginning 7 days prior to bleomycin-mediated injury resulted in reduced fibrosis at day 21 post-insult.<sup>3</sup> These findings are consistent with studies from other laboratories in which uPA delivered systemically (in a dog model), through intratracheal administration (in a rat model), or via daily aerosolization for 10 treatments (in a rabbit model) significantly reduced bleomycin-induced collagen accumulation.<sup>4–6</sup> Restoring the balance of uPA and PAI-1 through the targeted deletion of the PAI-1 gene also reduces lung fibrosis in several different murine models.<sup>7–10</sup> Despite this tight relationship between uPA and PAI-1 and the severity of fibrosis, the specific mechanisms that drive collagen accumulation have not been fully elucidated.

Fibrosis is characterized by the excessive deposition of extracellular matrix (ECM), including collagen and fibronectin, and the accumulation of activated myofibroblasts with an apoptosis-resistant phenotype.<sup>11,12</sup> Mechanically, fibrotic lung tissue is characterized by decreased compliance/increased stiffness.<sup>13</sup> It has been well-established that cell–matrix interactions are critical to the regulation of fibroblast phenotypes, and that exposure to substrates with the stiffness of fibrotic lung parenchyma is sufficient to promote a change in fibroblast phenotype and a resistance to apoptosis.<sup>14–17</sup> Myofibroblasts on stiff ECM substrates elaborate increased amounts of PAI-1.<sup>18</sup> Linking PAI-1 with myofibroblast resistance to apoptosis, we have shown that plasminogen activation (mediated by endogenous uPA) induces fibroblast apoptosis in concert with pericellular fibronectin proteolysis, and that the profibrotic cytokine transforming growth factor (TGF)- $\beta$  inhibits this apoptosis by increasing PAI-1 production by the myofibroblasts.<sup>19</sup>

The link between alterations in plasminogen activation, fibroblast apoptosis, and lung fibrosis led us to hypothesize that enhancing intrapulmonary plasminogen activation would promote the resolution of established lung fibrosis and that this would be associated with an increase in myofibroblast apoptosis. Additionally, we sought to determine whether the effects of enhanced plasminogen activation on fibrosis would depend on the timing of delivery, and whether changes in lung collagen content would be accompanied by changes in

lung stiffness during the evolution and resolution of lung fibrosis. To test this hypothesis, we employed transgenic mice that overexpress uPA in the lung in a doxycycline-conditional manner.<sup>3</sup> These mice were subjected to bleomycin-induced lung injury and doxycycline administration was initiated at time points that allowed for assessments of the effects of uPA during the initiation, progression, and resolution phases of fibrosis in this model.<sup>20,21</sup> We found that throughout the course of lung injury and repair, uPA overexpression significantly reduced fibrosis. Importantly, uPA overexpression enhanced the resolution of established lung fibrosis in this model, and the reduction in lung collagen was associated with a reduction in the stiffness of lung parenchyma. Notably, uPA overexpression in fibrotic lungs was associated with an increase in myofibroblast apoptosis and restoration of alveolar epithelial cell homeostasis but had no significant impact in the inflammatory cell populations in the lung.

Current therapies for lung fibrosis are limited, and the few Food and Drug Administration-approved medications slow the decline in lung function but do not reverse the disease.<sup>22</sup> Our discovery that the upregulation of plasminogen activation in the alveolar space is sufficient to reverse established fibrosis provides motivation to test this approach in patients with fibrotic lung disorders.

## Methods

### Transgenic mice:

To allow for inducible lung-specific uPA overexpression, double transgenic mice possessing tetO-muPA and CCSP-rtTA gene constructs (designated “uPA”) were generated as previously described.<sup>3</sup> Control mice included littermates that possessed either one or none of the transgenes.

### Assessment of mouse genotypes:

The genotypes of the transgenic mice were determined as previously described.<sup>3</sup> Briefly, the presence/absence of the tetO-muPA construct was determined using polymerase chain reaction (PCR) reaction with primers that distinguished this transgene from the native uPA gene. The tetO-muPA primer sequences are as follows: upper primer 5-CTCTGCAACAGAGTCGT CAAATGGAGG-3, lower primer 5-CGGGGGAGGGGCAAACAACAGATGGCTGGC-3; product size 324 base pair (bp). To identify the presence/absence of the CCSP-rtTA construct the following primer sequences were employed: upper primer 5 ACTGCCCATGCCCCAACAC-3, lower primer 5-AAAATCTTGCCAGCTTTCCCC-3; product size 525 bp. The PCR conditions were the same for each primer pair as follows: 90°C for 1 minute followed by annealing at 62°C for 2 minutes followed by elongation at 72°C for 2 minutes. This temperature sequence was repeated for 30 cycles.

### Bleomycin treatment:

Weight- and age-matched (18–22 g at 6–8 weeks of age) transgenic mice and littermate controls were administered intratracheal bleomycin (1.15 u/kg in 50 µL of sterile phosphate-

buffered saline [PBS]; Sigma Chemical, St. Louis, Missouri, United States) as previously described.<sup>8,23</sup>

### **Doxycycline treatment:**

Mice were exposed to doxycycline (Sigma Chemical) by adding the antibiotic to their drinking water at a concentration of 0.5 mg/mL in 1% ethanol. The doxycycline solution was protected from light using amber bottles, and the solution was changed every other day during the course of each study. Mice were assessed every other day following bleomycin administration for excessive weight loss and/or moribund status, and no animals required euthanasia prior to the designated experimental endpoints. For the prevention study, doxycycline was administered from day 1 through day 28. For the late inflammatory and early fibrotic phase study, doxycycline was administered from day 9 or day 14 through day 28. For the reversal study, doxycycline was administered from day 21 through day 42. For direct comparisons of early versus late transgene expression and the assessments of fibrosis, alveolar epithelial cell homeostasis, and lung inflammation, doxycycline was administered either from day 0 to 14 or from day 14 to 28.

### **Lung histology:**

The left lung was inflation-fixed at 25 cm H<sub>2</sub>O pressure with 10% neutral-buffered formalin, removed en bloc, further fixed in 10% neutral-buffered formalin overnight, and then paraffin embedded. Five micron sections were stained using hematoxylin and eosin or picosirius red.<sup>24</sup>

### **Hydroxyproline assay:**

Hydroxyproline content of the lung was measured using both lungs of each mouse included in the analysis (the individual “n” for each experimental condition is included within the figure) as previously described.<sup>3</sup> Each data point demonstrates the hydroxyproline content of a separate mouse included in the study.

### **Atomic force microscopy:**

Atomic force microscopy (AFM) was done as previously described.<sup>25</sup> Briefly, lungs were harvested, inflated with OCT, and cryosectioned to 50- to 60- $\mu$ m thick tissue strips. Tissue strips were attached to a glass slide and then mechanically characterized using an AFM (MFP-3D; Asylum Research or Catalyst Bioscope; Bruker) in PBS at room temperature by performing microindentation using a sphere-tipped probe (Novascan) with a diameter of 5  $\mu$ m and a spring constant of approximately 60 to 100 pN/nm. Force-indentation profiles were acquired by sampling sections of lung tissue using AFM microindentation with an indentation rate of 20  $\mu$ m/s and a spherical tip indenter of 5  $\mu$ m diameter.<sup>25,26</sup> Multiple regions were analyzed from each lung with the exclusion of large airways and vessels. The shear modulus was calculated by fitting each force-indentation profile using a Hertz sphere model. Figures include individual shear modulus values from one force curve and all measurements have been pooled, as in previous reports, to demonstrate the distribution within each cohort.<sup>18,25</sup> The number of mice from which the data are pooled for each cohort is indicated within the figures.

## Immunohistochemistry and Terminal Deoxynucleotidyl Transferase dUTP Nick End Labeling Staining

Lungs were perfused with PBS, inflated with intratracheal OCT, removed, and immediately frozen in a dry-ice alcohol bath. Lungs were stored at  $-80^{\circ}\text{C}$ . Ten-micron lung sections were stained as previously described.<sup>27</sup> Briefly, lung sections were fixed in 3.7% paraformaldehyde, permeabilized with 0.5% Triton, and blocked with 5% goat serum and 1% bovine serum albumin in PBS. The slides were stained with primary fluorescein isothiocyanate (FITC)-conjugated anti-smooth muscle antibody (SMA) or FITC-conjugated antibody to surfactant protein C (SPC) and costained with terminal deoxynucleotidyl transferase dUTP nick end labeling (TUNEL) by using the In Situ Cell Death Detection Kit TMR Red (Roche). Slides were mounted in Prolong Gold containing 4',6-diamidino-2-phenylindole (Molecular Probes). Stained sections were visualized on an Olympus BX-51 fluorescence microscope (Olympus, Tokyo, Japan), and images were captured with an Olympus DP-70 camera and analyzed with DP controller software version 3.1.1.267. Quantification of double-positive cells (TUNEL+/ $\alpha$ -SMA+ or TUNEL+/ $\alpha$ -SPC+) was done by investigators who were blinded to the genotype and treatment cohorts. Representative examples of cells that were counted as double-positive are shown in ►Fig. 6 (TUNEL+/ $\alpha$ -SMA+) and ►Supplementary Fig. S1 (TUNEL+/ $\alpha$ -SPC+) (available in the online version). Ten separate high-powered fields were assessed from each of two mice per cohort.

### Tissue collection for lung leukocyte quantification:

Lungs were perfused via the right heart using PBS containing 0.5 mM ethylenediaminetetraacetic acid until pulmonary vessels were grossly clear. Lungs were then excised, minced, and enzymatically digested to obtain a single cell suspension of lung leukocytes as previously described.<sup>28</sup>

### Antibody staining and flow cytometric analysis:

Staining, including blockade of Fc receptors, and analysis by flow cytometry was performed as described previously.<sup>28</sup> Flow cytometry was performed on either a Becton Dickinson (BD) LSR II or a BD LSR Fortessa (BD Biosciences), utilizing 12 photomultiplier tube channels. After gating out debris and doublets, a total of 100,000 events were acquired from each sample using FACSDiva data acquisition software. Data were analyzed using FlowJo software (Treestar, Ashland, Oregon, United States). Specific populations of CD45+ leukocytes including neutrophils and alveolar and exudate macrophages were identified as previously described.<sup>29</sup>

### Statistical Analysis

All data were analyzed by an ordinary one-way analysis of variance with Tukey's multiple comparison testing using GraphPad Prism version 7.03 (GraphPad Software, Inc., San Diego, California, United States) and displayed as the mean with standard error of the mean. Each point represents a unique measurement. *p*-Values of  $< 0.05$  were considered statistically significant. Sample size and replicates for each experiment are included within the corresponding figure.

## Results

### Early uPA overexpression prevents lung fibrosis:

We previously demonstrated that doxycycline treatment of tetO-muPA:CCSP-rtTA (uPA) double transgenic mice induced bronchoalveolar lavage (BAL) fluid uPA expression after 7 and 14 days of exposure, and that doxycycline-mediated uPA expression persisted even after bleomycin-induced injury.<sup>3,30</sup> Additionally, we previously showed that in the absence of doxycycline, there was no uPA expression indicating that the transgenic system exhibited no detectable leak. We also found that the administration of doxycycline induced alveolar compartment uPA activity in the double transgenic mice within 12 hours of doxycycline exposure, with peak expression observed after 48 hours of exposure.<sup>30</sup> With the cessation of doxycycline, uPA activity diminished over 12 to 24 hours and was undetectable at 48 hours.

To examine the impact of uPA overexpression during the initiation phase of lung injury on the development of lung fibrosis, tetO-muPA:CCSP-rtTA (uPA) double transgenic mice and littermate control mice were administered intratracheal bleomycin or an equal volume of saline (defined as day 0). We then initiated doxycycline in all mice (transgenic and littermate controls) beginning 24 hours later (day 1). At day 28, lung hydroxyproline quantification confirmed that uPA overexpression initiated during the early inflammatory phase of lung injury and continuing through the fibrotic phase of the bleomycin model prevented the lung collagen accumulation representative of fibrosis (►Fig. 1). Measurement of lung parenchymal stiffness using AFM showed that there was no difference between the uninjured double transgenic uPA mice and their littermate controls after 27 days of doxycycline administration (►Supplementary Fig. S2A, available in the online version). In contrast, the littermate control mice that received intratracheal bleomycin had a substantial increase in lung stiffness at day 28, while the transgenic mice with acute lung injury that did not develop fibrosis had no difference in lung stiffness compared with either the PBS-treated uPA group or the PBS-treated littermate controls (►Supplementary Fig. S2A, available in the online version).

### uPA overexpression in the late-inflammatory phase diminishes lung fibrosis:

Having shown that increased intrapulmonary uPA expression beginning in the early injury/inflammatory phase of the bleomycin model prevents the development of lung fibrosis, we next sought to examine the impact of uPA overexpression during the late-inflammatory/early fibrotic phase. In this set of experiments, transgenic uPA mice and littermate controls were administered intratracheal bleomycin or PBS (day 0), and doxycycline was administered from days 9 through 28 (►Fig. 2). With the induction of uPA expression after the peak of inflammation (i.e., day 7), we again observed a significant reduction in lung collagen (►Fig. 2) and an associated normalization of parenchymal lung stiffness (►Supplementary Fig. S2B, available in the online version) in the uPA cohort.

### uPA overexpression during the early fibrotic phase diminishes lung fibrosis:

The upregulation of uPA in the lungs during the early or late inflammatory phase following lung injury attenuated lung fibrosis, so we next sought to determine whether uPA induction

could alter the course of established lung fibrosis. Studies in the bleomycin model have demonstrated that new collagen synthesis peaks around day 14, after which the rate of new collagen synthesis progressively declines toward baseline rates.<sup>31,32</sup> To assess the effect of enhanced uPA expression during the fibrotic phase of the bleomycin model, we injured the uPA double transgenic mice and littermate controls with intratracheal bleomycin at day 0. We compared lung collagen content between these groups (in the absence of doxycycline) at day 14 and found significant elevations compared with baseline ( $p < 0.01$  for each, data not shown), but there was no difference in lung hydroxyproline between the two groups (►Fig. 3A). In separate cohorts, doxycycline was administered from days 14 to 28. At day 28, the bleomycin-injured uPA mice had significantly decreased lung collagen compared with littermate controls (►Fig. 3B). The induction of intrapulmonary uPA expression was, again, associated with a reduction in parenchymal stiffness following bleomycin (►Supplementary Fig. S2C, available in the online version). The significant decrease in lung fibrosis was also evident on histology (►Fig. 3C).

### **uPA overexpression reduces alveolar-capillary leak without impacting inflammation or type 2 AEC homeostasis:**

To distinguish the effects of uPA overexpression during the inflammatory phase of the bleomycin model from the effects of uPA overexpression during the fibrotic phase, we designed an experiment in which mice received doxycycline to induce uPA overexpression either from days 1 to 14 or from days 14 to 28 following intratracheal bleomycin, and we assessed lung collagen content in both cohorts at day 28 (►Fig. 4A and B). Notably, in each experimental protocol we observed a significant reduction in lung collagen content, suggesting that uPA upregulation can limit the development of lung fibrosis during the early phase of lung injury while inflammation is prevalent and also in the postinflammatory phase of lung injury and repair.

Next, to evaluate the impact of uPA expression on alveolar epithelial cell injury and homeostasis in this model, and to assess the effects on inflammatory cell accumulation, we used a similar study design with intratracheal bleomycin (or PBS) at day 0 and administration of doxycycline for 7 days early following injury (days 1–7) or late (days 14–21). At day 7 in the “early” protocol and day 21 in the “late” protocol, we obtained alveolar lavage fluid for assessment of inflammatory cell numbers (►Supplementary Fig. S3, available in the online version) and measurement of albumin as an indicator of alveolar–capillary barrier dysfunction (►Fig. 4C and D). We also obtained serum at the same time points for the measurement of surfactant protein D (SP-D; ►Fig. 4E and F) as a surrogate for type 2 alveolar epithelial cell homeostasis. With both the early and late overexpression of uPA, we observed a significant decrease in albumin within the alveolar lavage fluid although this was not associated with a significant reduction in serum SP-D. Additionally, we observed no significant difference in the inflammatory cell populations (total CD45+ cells, neutrophils, alveolar macrophages, or exudative macrophages) in the lung in response to early or late uPA overexpression (►Supplementary Fig. S3, available in the online version).

### **uPA overexpression facilitates the resolution of established lung fibrosis:**

In the next set of experiments, we examined the impact of increased intrapulmonary uPA expression on the resolution phase of established lung fibrosis. In the uninjured uPA and littermate control groups, the baseline levels of hydroxyproline were similar at days 21 and 42 (►Fig. 5A; PBS). We then compared hydroxyproline content in bleomycin-injured littermate controls and uPA double transgenic mice at day 21 (prior to the initiation of doxycycline), and found that there was a significant increase compared with uninjured animals ( $p < 0.0001$ ). Importantly, on day 21, the increase in lung hydroxyproline following bleomycin was not different between the littermate controls and the transgenic mice (►Fig. 5A; Bleo-day 21). Following doxycycline exposure from day 21 through day 42, the bleomycin-injured uPA mice had significantly decreased collagen content compared with the littermate control group. Furthermore, the day 42 lung collagen content in the double transgenic group was significantly reduced compared with the day 21 level (►Fig. 5A; Bleo-day 42). In contrast, the bleomycin-injured littermate control group had no significant change in hydroxyproline between day 21 and day 42 with doxycycline exposure. Measures of lung parenchymal stiffness correlated with lung hydroxyproline, showing that the uPA mice had a significant decline in shear modulus at day 42 compared with the day 42 bleomycin-treated littermate controls (►Fig. 5B). The average parenchymal stiffness for the individual mice is shown in ►Supplementary Fig. S4 (available in the online version). To further evaluate the fibrotic response in the different groups, histology sections were prepared from bleomycin-injured uPA and wild-type mice at day 21 (prior to administration of doxycycline) and day 42 (following the 21 days of doxycycline administration). Hematoxylin and eosin staining was done on days 21 and 42 lungs (►Fig. 5C) and picrosirius red staining was done on the day 42 lungs (►Fig. 5D). Consistent with the hydroxyproline results, we observed no difference between the two groups at day 21 with alveolar wall thickening and increased cellularity (typical of bleomycin-induced fibrosis) present in both groups. At day 42, using picrosirius to stain for lung collagen, we detected increased areas of fibrosis in the wild-type mice compared with the uPA transgenic mice.

### **uPA overexpression enhances myofibroblast apoptosis:**

Prior studies from our laboratory and others have shown that antifibrotic interventions in murine models of lung fibrosis are associated with increased evidence of myofibroblast apoptosis *in vivo*<sup>24,33–35</sup> and that plasminogen activation promotes fibroblast apoptosis *in vitro*.<sup>19,36</sup> To explore whether the enhanced resolution of established fibrosis due to uPA overexpression was associated with increased myofibroblast apoptosis, we examined lungs from uPA overexpressing mice and littermate controls at day 24 following bleomycin administration (3 days after initiation of doxycycline). The lungs were stained with TUNEL for detection of apoptotic cells and costained with either  $\alpha$ -SMA for detection of differentiated myofibroblasts or with SPC to detect type 2 alveolar epithelial cells. Images were obtained from 10 randomly selected sections in the lungs of two mice per cohort. Cells that stained “double-positive” for TUNEL and  $\alpha$ -SMA or TUNEL and SPC were quantified by an investigator blinded to both the genotype and treatment cohort. We detected more than a twofold increase in the number of apoptotic myofibroblasts in the uPA overexpressing mice compared with the littermate controls (►Fig. 6). In contrast, there were no significant



changes in the number of apoptotic alveolar epithelial cells (►Fig. 6C and ►Supplementary Fig. S1, available in the online version).

## Discussion

Lung fibrosis represents a common endpoint of both acute and chronic injuries to the alveolus, and progressive scarring is thought to result from an aberrant wound repair response.<sup>11</sup> Key characteristics of lung fibrosis, regardless of etiology, include the accumulation and persistent activation of myofibroblasts, increased lung collagen content, the development of a rigid ECM, and evidence of type 2 alveolar epithelial cell dysfunction. Although the capacity of lung to “resolve” established fibrosis has not been clearly demonstrated or rigorously studied, successful resolution of established scar is likely to require both ECM degradation and clearance of myofibroblasts via apoptosis.<sup>11,37</sup> We have previously determined in *in vitro* studies that enhanced plasminogen activation promotes ECM fibronectin degradation and fibroblast apoptosis.<sup>19</sup> Based on this observation coupled with prior studies from our laboratory and others demonstrating that an imbalance of PAs and PAI-1 is critical for the establishment of lung fibrosis,<sup>1</sup> we hypothesized that upregulating intrapulmonary plasminogen activation would promote the reversal of established fibrosis and that this resolution would coincide with an increase in myofibroblast apoptosis. Using the bleomycin model of lung fibrosis and transgenic mice with inducible alveolar uPA expression, we conclusively demonstrate that increased intrapulmonary plasminogen activation promotes the resolution of lung fibrosis and that this resolution is accompanied by a reduction in lung parenchymal stiffness and an increase in fibroblast apoptosis.

Several studies have identified an impairment in intrapulmonary fibrinolysis in patients with acute and chronic fibrotic lung diseases including acute respiratory distress syndrome and diffuse interstitial lung disease.<sup>38,39</sup> This imbalance results from an increased expression of PAI-1 relative to the PAs (i.e., uPA and tPA). Studies in which the intrapulmonary levels of uPA are restored through either exogenous administration or enhanced gene expression have firmly established a causal role for this uPA/PAI-1 imbalance in the development of lung fibrosis. Notably, the protection against fibrosis that results from increasing intrapulmonary uPA levels appears to occur with both early and late intervention after bleomycin injury. For example, our laboratory demonstrated that increasing intrapulmonary uPA levels via adenoviral-mediated gene delivery on day 21 after bleomycin, a time point when fibrosis is well established, reduced the level of lung collagen content on day 28.<sup>2</sup> Similar findings were reported by Günther et al who showed that the delivery of uPA via aerosol between days 14 and 24 reduced lung hydroxyproline concentration, improved lung histology, and restored lung compliance on day 28 in bleomycin-injured rabbits.<sup>6</sup> The same study established that early administration of uPA (i.e., from days 2 to 12) also significantly reduced day 28 lung hydroxyproline levels. However, the early treatment had a diminished effect on lung compliance, suggesting that the protective effect of uPA was more robust during the fibrotic phase of the model. We demonstrate consistent findings in this study, showing that overexpression of uPA between days 1 and 14 or between days 14 and 28 had similar effects on lung collagen content at day 28. These prior studies, in conjunction with our current work, suggest that intrapulmonary uPA can inhibit fibrogenesis through actions

during the early inflammatory phase following lung injury, and also clearly demonstrate that uPA has beneficial antifibrotic activity when present in the postinflammatory phase following injury. Notably, the prior studies did not establish whether increasing intrapulmonary uPA levels simply prevent progressive collagen deposition or whether they actually reverse established fibrosis. In the present study, we clearly demonstrate the reversal of existing fibrosis by documenting that control and uPA overexpressing transgenic mice have similar levels of lung collagen at day 21 prior to the initiation of doxycycline, and that from days 21 to 42 there is a significant decline in lung collagen in the transgenic group with the induction of uPA expression. The improvement in fibrosis contrasts with the stable (or slightly increased) quantities of lung collagen observed in the controls over this same time interval.

The mechanisms by which restoring the balance between PAs and PAI-1 reduces lung fibrosis have not been firmly established. Our current study suggests that the mechanisms involved may be different depending on when, during the evolution of lung injury and fibrosis, uPA levels are enhanced. We found that whether uPA was overexpressed early or late following injury there was a decrease in alveolar–capillary leak without a change in serum SP-D or the inflammatory cell populations in the lung. This suggests that uPA overexpression has a concomitant role in maintenance of the alveolar epithelial barrier function, which may be related to the role of plasminogen activation in alveolar epithelial cell migration.<sup>40</sup> Additionally, this study implicates a mechanism whereby uPA overexpression in the context of established fibrosis can facilitate the apoptotic elimination of myofibroblasts, promote collagen degradation, and enhance the restoration of normal lung architecture.

The classic function of plasminogen following its activation to plasmin is to degrade fibrin, and early studies hypothesized that fibrin accumulation was a critical intermediary for the development of fibrosis. However, we found that mice deficient in fibrin(ogen) develop a similar severity of lung fibrosis when compared with wild-type animals following lung injury, suggesting that the role of plasminogen activation in fibrosis extends beyond fibrinolysis.<sup>8,41,42</sup> Although fibrin removal does not appear to be critical in mitigating collagen accumulation, the importance of plasmin as an antifibrotic mediator is supported by studies from our laboratory. We specifically demonstrated that inhibition of plasmin with tranexamic acid reversed the protective effects of PAI-1 deficiency following bleomycin-induced lung injury.<sup>8</sup> Plasmin possesses several functional activities besides fibrin degradation that could contribute to its antifibrotic activity including hepatocyte growth factor (HGF) activation.<sup>23,43</sup>

Another potential mechanism by which plasminogen activation might modulate lung fibrosis is through its regulation of fibroblast survival. Specifically, *in vitro* studies from our laboratory have demonstrated that treatment of fibroblasts with plasminogen resulted in a significant increase in apoptosis in conjunction with the proteolytic degradation of the ECM protein fibronectin.<sup>19</sup> Exposure of wild-type lung fibroblasts to the profibrotic growth factor TGF- $\beta$ 1 significantly blunted plasminogen-mediated apoptosis and fibronectin degradation as a result of the increased lung fibroblast PAI-1 expression and the resultant inhibition of plasminogen activation. Indeed, fibroblasts from patients with fibrotic lung disease had

increased resistance to plasminogen-induced apoptosis due to constitutively increased secretion of PAI-1.<sup>36</sup> Complementary studies from other laboratories have confirmed the importance of plasmin-mediated proteolysis of the ECM in the regulation of apoptosis of different cell types including Chinese hamster ovary cells, vascular smooth muscle cells, and valvular myofibroblasts.<sup>44–46</sup> Based on these in vitro data, it is tempting to conclude that the induction of intrapulmonary uPA expression in the present study leads to a restoration of plasminogen activation which in turn enhances ECM proteolysis and causes fibroblast apoptosis. Consistent with this conclusion, we did observe an increase in the numbers of TUNEL/ $\alpha$ -SMA (but not TUNEL/SPC) double positive cells following the initiation of uPA expression providing further support for the link between myofibroblast apoptosis and fibrosis resolution. However, our current study does not definitively establish this mechanism. The identification and quantification of apoptosis in vivo is challenging for several reasons. First, apoptosis is a dynamic process while our quantification is necessarily a snapshot assessment at a single point in time. Second, this snapshot is affected by the rate of apoptotic cell removal from the injured tissue via efferocytosis and other clearance mechanisms. Finally, our quantification is based on identifying cells that are positive for both nuclear TUNEL staining and for cytoplasmic expression of  $\alpha$ -SMA, but during the evolution of apoptosis,  $\alpha$ -SMA and other cytoskeletal proteins are catabolized.

As an alternative mechanism by which increased plasminogen activation reduces fibrosis, we have also shown that the intrapulmonary administration of uPA increases the level of HGF in BAL fluid, and HGF itself has been implicated in fibroblast apoptosis.<sup>43,47</sup> It is also important to mention that our results contradict a recent report which found uPA, through its generation of plasmin and the downstream activation of protease-activated receptor-1 signaling and interleukin (IL)-6, to function as a profibrotic molecule.<sup>48</sup> In that study, the investigators observed increased uPA expression in the epithelium and myofibroblasts of idiopathic pulmonary fibrosis (IPF) lung tissue, increased uPA in the serum of IPF patients, and an inverse correlation between serum uPA and lung function in patients with IPF. Moreover, treatment of fibroblasts with doses of plasminogen that are lower than those that induce apoptosis were found to promote proliferation through activation of IL-6. It is possible, in light of these findings, that the robust uPA expression demonstrated in the IPF lung tissue may be a reactive response to the impaired plasminogen activation, or is overwhelmed by the excessive PAI-1. In either case, our studies indicate that the net effect of uPA activation is antifibrotic.

The lung fibrosis that results from a single intratracheal dose of bleomycin is often described as self-limited and spontaneously resolving, and this characteristic among others is said to distinguish this model from the insidiously progressive scarring that occurs in IPF.<sup>21</sup> However, a publication commonly cited to substantiate the reversibility of bleomycin injury assessed fibrosis endpoints at day 14 and day 21, and the reported hydroxyproline level at day 21 was greater than day 14.<sup>49</sup> In contrast to this dictum of reversibility, we find that bleomycin-induced fibrosis (as defined by lung collagen content and parenchymal stiffness) persists in control mice at least through day 42. These results are consistent with the classic report of Bakowska and Adamson who observed a steady increase in lung collagen content (as measured by hydroxyproline) through day 56 after bleomycin instillation.<sup>50</sup> Although neither we nor Bakowska and Adamson investigated the fate of fibrosis beyond the day 42 or

day 56 time points, Hecker et al found that young mice (8 weeks) have less total lung hydroxyproline at day 112 when compared with day 21 after bleomycin, suggesting that, at some time point between day 42 and day 112, fibrosis does regress.<sup>34</sup> However, this capability of mice to resolve their bleomycin-induced fibrosis is influenced by age because old mice (18 months) exhibited minimal improvement of their lung collagen content between day 21 and day 112. Beyond the effect of animal age on the reversibility of fibrosis, interpretation of the reversibility of the bleomycin model is also likely to be influenced by the measured endpoints in a study. For example, Schiller et al demonstrated a return to baseline of lung compliance by day 28 after bleomycin, and they also observed an improvement (but not complete reversion) of lung histologic changes.<sup>51</sup> Similarly, a recent study reported that, in a model of tumor necrosis factor (TNF)- $\alpha$  overexpression-induced fibrosis, a significant elevation in lung hydroxyproline persisted 4 weeks after discontinuation of TNF- $\alpha$  overexpression compared with baseline despite the marked decline in the histologic abnormalities and the apparent resolution of fibrotic changes visualized by lung magnetic resonance imaging.<sup>52</sup> The discordance between hydroxyproline, lung histology, and lung compliance when analyzing the regression of fibrosis may relate to confounding factors including tissue cellularity, tissue edema, and collagen maturation. Collectively, these studies highlight the value of combined biochemical, physiologic, and histologic endpoints.<sup>13,21</sup>

Recent studies have shown that increased lung stiffness can support myofibroblast differentiation, survival, and PAI-1 expression through transcriptional responses mediated by the HIPPO pathway and/or nuclear localization of myocardin-related transcription factor-A.<sup>14,18,24</sup> Importantly, increased tissue stiffness is not merely a consequence of collagen accumulation and fibrosis, as increased stiffness has been shown to precede measurable increases in collagen levels in models of liver fibrosis.<sup>53</sup> Moreover, activation of mechanotransduction signaling pathways seems to directly contribute to the maintenance and progression of the myofibroblast phenotype and lung fibrosis.<sup>12,14,16,18,24,54</sup> Importantly, in the current study we hypothesized that a reduction in lung fibrosis would coincide with a reduction in lung stiffness coupled with increased fibroblast apoptosis. Our data clearly support this hypothesis, as changes in lung stiffness strongly correlated with the development, and resolution of lung fibrosis. We have recently demonstrated that estimates of lung stiffness using transthoracic ultrasound can be achieved, suggesting that noninvasive imaging may feasibly serve as a surrogate measure for longitudinal changes in fibrosis in patients with acute lung injury and, possibly, other etiologies of lung fibrosis.<sup>55</sup> Such noninvasive assessments of liver<sup>56</sup> and bowel stiffness<sup>57,58</sup> have been used as surrogates for fibrosis in other organs, and development of noninvasive direct measures of lung stiffness could have translational potential for the assessment of lung fibrosis and treatment efficacy.

In conclusion, our study demonstrates that uPA overexpression can prevent the development of lung fibrosis and can promote the resolution of established lung fibrosis which is coupled with evidence of increased myofibroblast apoptosis. We additionally show that changes in lung stiffness, as assessed by AFM, reflect the development and regression of lung fibrosis. Further studies are warranted to: (1) define the mechanism by which uPA promotes fibrosis regression and (2) determine whether this is mediated by increased plasminogen activation or through mechanisms independent of plasminogen proteolysis. Finally, our study

demonstrates that when fibrosis is established, changes in lung stiffness correlate with the decline in lung collagen, suggesting the utility of lung stiffness as a physiologic correlate of lung fibrosis resolution.

## Supplementary Material

Refer to Web version on PubMed Central for supplementary material.

## Funding

Funding for this project was provided by NIH HL105489 and 141195 (to J.C.H.), HL078871 (to T.H.S.), HL108904 (to K.K.K.), HL092961 and HL133320 (to D.J.T.), and Department of Defense GW160154 (to J.J.O.).

## References

1. Sisson TH, Simon RH. The plasminogen activation system in lung disease. *Curr Drug Targets* 2007;8(09):1016–1029 [PubMed: 17896953]
2. Sisson TH, Hattori N, Xu Y, Simon RH. Treatment of bleomycin-induced pulmonary fibrosis by transfer of urokinase-type plasminogen activator genes. *Hum Gene Ther* 1999;10(14):2315–2323 [PubMed: 10515451]
3. Sisson TH, Hanson KE, Subbotina N, Patwardhan A, Hattori N, Simon RH. Inducible lung-specific urokinase expression reduces fibrosis and mortality after lung injury in mice. *Am J Physiol Lung Cell Mol Physiol* 2002;283(05):L1023–L1032 [PubMed: 12376355]
4. Ikeda T, Hirose N, Koto H, Hirano H, Shigematsu N. Fibrin deposition and fibrinolysis in the pathogenesis of pulmonary fibrosis [in Japanese]. *Nihon Kyobu Shikkan Gakkai Zasshi* 1989; 27(04):448–451 [PubMed: 2796052]
5. Hart DA, Whidden P, Green F, Henkin J, Woods DE. Partial reversal of established bleomycin-induced pulmonary fibrosis by rh-urokinase in a rat model. *Clin Invest Med* 1994;17(02):69–76 [PubMed: 7516275]
6. Günther A, Lübke N, Ermert M, et al. Prevention of bleomycin-induced lung fibrosis by aerosolization of heparin or urokinase in rabbits. *Am J Respir Crit Care Med* 2003;168(11):1358–1365 [PubMed: 14644925]
7. Eitzman DT, McCoy RD, Zheng X, et al. Bleomycin-induced pulmonary fibrosis in transgenic mice that either lack or overexpress the murine plasminogen activator inhibitor-1 gene. *J Clin Invest* 1996;97(01):232–237 [PubMed: 8550840]
8. Hattori N, Degen JL, Sisson TH, et al. Bleomycin-induced pulmonary fibrosis in fibrinogen-null mice. *J Clin Invest* 2000;106(11): 1341–1350 [PubMed: 11104787]
9. Courey AJ, Horowitz JC, Kim KK, et al. The vitronectin-binding function of PAI-1 exacerbates lung fibrosis in mice. *Blood* 2011; 118(08):2313–2321 [PubMed: 21734232]
10. Osterholzer JJ, Christensen PJ, Lama V, et al. PAI-1 promotes the accumulation of exudate macrophages and worsens pulmonary fibrosis following type II alveolar epithelial cell injury. *J Pathol* 2012;228(02):170–180 [PubMed: 22262246]
11. Glasser SW, Hagood JS, Wong S, Taype CA, Madala SK, Hardie WD. Mechanisms of lung fibrosis resolution. *Am J Pathol* 2016;186(05):1066–1077 [PubMed: 27021937]
12. Horowitz JC, Thannickal VJ. Mechanisms for the resolution of organ fibrosis. *Physiology (Bethesda)* 2019;34(01):43–55 [PubMed: 30540232]
13. Thannickal VJ, Henke CA, Horowitz JC, et al. Matrix biology of idiopathic pulmonary fibrosis: a workshop report of the national heart, lung, and blood institute. *Am J Pathol* 2014;184(06):1643–1651 [PubMed: 24726499]
14. Zhou Y, Huang X, Hecker L, et al. Inhibition of mechanosensitive signaling in myofibroblasts ameliorates experimental pulmonary fibrosis. *J Clin Invest* 2013;123(03):1096–1108 [PubMed: 23434591]

15. Booth AJ, Hadley R, Cornett AM, et al. Acellular normal and fibrotic human lung matrices as a culture system for in vitro investigation. *Am J Respir Crit Care Med* 2012;186(09):866–876 [PubMed: 22936357]
16. Parker MW, Rossi D, Peterson M, et al. Fibrotic extracellular matrix activates a profibrotic positive feedback loop. *J Clin Invest* 2014;124(04):1622–1635 [PubMed: 24590289]
17. Dodi AE, Ajayi IO, Chang C, et al. Regulation of fibroblast Fas expression by soluble and mechanical pro-fibrotic stimuli. *Respir Res* 2018;19(01):91 [PubMed: 29747634]
18. Liu F, Lagares D, Choi KM, et al. Mechanosignaling through YAP and TAZ drives fibroblast activation and fibrosis. *Am J Physiol Lung Cell Mol Physiol* 2015;308(04):L344–L357 [PubMed: 25502501]
19. Horowitz JC, Rogers DS, Simon RH, Sisson TH, Thannickal VJ. Plasminogen activation induced pericellular fibronectin proteolysis promotes fibroblast apoptosis. *Am J Respir Cell Mol Biol* 2008; 38(01):78–87 [PubMed: 17656680]
20. Blackwell TS, Tager AM, Borok Z, et al. Future directions in idiopathic pulmonary fibrosis research. An NHLBI workshop report. *Am J Respir Crit Care Med* 2014;189(02):214–222 [PubMed: 24160862]
21. Jenkins RG, Moore BB, Chambers RC, et al.; ATS Assembly on Respiratory Cell and Molecular Biology. An Official American Thoracic Society Workshop Report: use of animal models for the preclinical assessment of potential therapies for pulmonary fibrosis. *Am J Respir Cell Mol Biol* 2017;56(05):667–679 [PubMed: 28459387]
22. Raghu G, Rochwerf B, Zhang Y, et al.; American Thoracic Society; European Respiratory society; Japanese Respiratory Society; Latin American Thoracic Association. An Official ATS/ERS/JRS/ALAT Clinical Practice Guideline: treatment of idiopathic pulmonary fibrosis. An update of the 2011 clinical practice guideline. *Am J Respir Crit Care Med* 2015;192(02):e3–e19 [PubMed: 26177183]
23. Bauman KA, Wettlaufer SH, Okunishi K, et al. The antifibrotic effects of plasminogen activation occur via prostaglandin E2 synthesis in humans and mice. *J Clin Invest* 2010;120(06):1950–1960 [PubMed: 20501949]
24. Sisson TH, Ajayi IO, Subbotina N, et al. Inhibition of myocardin-related transcription factor/serum response factor signaling decreases lung fibrosis and promotes mesenchymal cell apoptosis. *Am J Pathol* 2015;185(04):969–986 [PubMed: 25681733]
25. Liu F, Mih JD, Shea BS, et al. Feedback amplification of fibrosis through matrix stiffening and COX-2 suppression. *J Cell Biol* 2010; 190(04):693–706 [PubMed: 20733059]
26. Sicard D, Fredenburgh LE, Tschumperlin DJ. Measured pulmonary arterial tissue stiffness is highly sensitive to AFM indenter dimensions. *J Mech Behav Biomed Mater* 2017;74:118–127 [PubMed: 28595103]
27. Yang J, Wheeler SE, Velikoff M, et al. Activated alveolar epithelial cells initiate fibrosis through secretion of mesenchymal proteins. *Am J Pathol* 2013;183(05):1559–1570 [PubMed: 24012677]
28. Osterholzer JJ, Olszewski MA, Murdock BJ, et al. Implicating exudate macrophages and Ly-6C(high) monocytes in CCR2-dependent lung fibrosis following gene-targeted alveolar injury. *J Immunol* 2013;190(07):3447–3457 [PubMed: 23467934]
29. Roussey JA, Viglianti SP, Teitz-Tennenbaum S, Olszewski MA, Osterholzer JJ. Anti-PD-1 antibody treatment promotes clearance of persistent cryptococcal lung infection in mice. *J Immunol* 2017; 199(10):3535–3546 [PubMed: 29038249]
30. Sisson TH, Hansen JM, Shah M, et al. Expression of the reverse tetracycline-transactivator gene causes emphysema-like changes in mice. *Am J Respir Cell Mol Biol* 2006;34(05):552–560 [PubMed: 16415250]
31. Blaauuboer ME, Emson CL, Verschuren L, et al. Novel combination of collagen dynamics analysis and transcriptional profiling reveals fibrosis-relevant genes and pathways. *Matrix Biol* 2013; 32(7–8):424–431 [PubMed: 23648810]
32. Raghov R, Lurie S, Seyer JM, Kang AH. Profiles of steady state levels of messenger RNAs coding for type I procollagen, elastin, and fibronectin in hamster lungs undergoing bleomycin-induced interstitial pulmonary fibrosis. *J Clin Invest* 1985;76(05): 1733–1739 [PubMed: 2414324]

33. Ashley SL, Sisson TH, Wheaton AK, et al. Targeting inhibitor of apoptosis proteins protects from bleomycin-induced lung fibrosis. *Am J Respir Cell Mol Biol* 2016;54(04):482–492 [PubMed: 26378893]
34. Hecker L, Logsdon NJ, Kurundkar D, et al. Reversal of persistent fibrosis in aging by targeting Nox4-Nrf2 redox imbalance. *Sci Transl Med* 2014;6(231):231ra47
35. Lagares D, Santos A, Grasberger PE, et al. Targeted apoptosis of myofibroblasts with the BH3 mimetic ABT-263 reverses established fibrosis. *Sci Transl Med* 2017;9(420):eaal3765 [PubMed: 29237758]
36. Chang W, Wei K, Jacobs SS, Upadhyay D, Weill D, Rosen GD. SPARC suppresses apoptosis of idiopathic pulmonary fibrosis fibroblasts through constitutive activation of beta-catenin. *J Biol Chem* 2010; 285(11):8196–8206 [PubMed: 20061390]
37. Zhou Y, Horowitz JC, Naba A, et al. Extracellular matrix in lung development, homeostasis and disease. *Matrix Biol* 2018;73:77–104 [PubMed: 29524630]
38. Idell S, James KK, Levin EG, et al. Local abnormalities in coagulation and fibrinolytic pathways predispose to alveolar fibrin deposition in the adult respiratory distress syndrome. *J Clin Invest* 1989;84(02):695–705 [PubMed: 2788176]
39. Prabhakaran P, Ware LB, White KE, Cross MT, Matthay MA, Olman MA. Elevated levels of plasminogen activator inhibitor-1 in pulmonary edema fluid are associated with mortality in acute lung injury. *Am J Physiol Lung Cell Mol Physiol* 2003;285(01):L20–L28 [PubMed: 12730079]
40. Lazar MH, Christensen PJ, Du M, et al. Plasminogen activator inhibitor-1 impairs alveolar epithelial repair by binding to vitronectin. *Am J Respir Cell Mol Biol* 2004;31(06):672–678 [PubMed: 15308506]
41. Chapman HA, Allen CL, Stone OL. Abnormalities in pathways of alveolar fibrin turnover among patients with interstitial lung disease. *Am Rev Respir Dis* 1986;133(03):437–443 [PubMed: 3954252]
42. Idell S, James KK, Gillies C, Fair DS, Thrall RS. Abnormalities of pathways of fibrin turnover in lung lavage of rats with oleic acid and bleomycin-induced lung injury support alveolar fibrin deposition. *Am J Pathol* 1989;135(02):387–399 [PubMed: 2476934]
43. Hattori N, Mizuno S, Yoshida Y, et al. The plasminogen activation system reduces fibrosis in the lung by a hepatocyte growth factor-dependent mechanism. *Am J Pathol* 2004;164(03): 1091–1098 [PubMed: 14982862]
44. Ho-Tin-Noé B, Meilhac O, Rossignol P, Lijnen HR, Anglés-Cano E. Dual effect of apolipoprotein(a) on plasmin(ogen)-induced apoptosis through modulation of cell detachment of adherent cells. *Thromb Haemost* 2006;95(01):142–150 [PubMed: 16543973]
45. Rossignol P, Ho-Tin-Noé B, Vranckx R, et al. Protease nexin-1 inhibits plasminogen activation-induced apoptosis of adherent cells. *J Biol Chem* 2004;279(11):10346–10356 [PubMed: 14699093]
46. Kochtebane N, Choqueux C, Passefort S, et al. Plasmin induces apoptosis of aortic valvular myofibroblasts. *J Pathol* 2010;221(01):37–48 [PubMed: 20186923]
47. Crestani B, Marchand-Adam S, Quesnel C, et al. Hepatocyte growth factor and lung fibrosis. *Proc Am Thorac Soc* 2012;9(03):158–163 [PubMed: 22802291]
48. Schuliga M, Jaffar J, Harris T, Knight DA, Westall G, Stewart AG. The fibrogenic actions of lung fibroblast-derived urokinase: a potential drug target in IPF. *Sci Rep* 2017;7:41770 [PubMed: 28139758]
49. Izbicki G, Segel MJ, Christensen TG, Conner MW, Breuer R. Time course of bleomycin-induced lung fibrosis. *Int J Exp Pathol* 2002; 83(03):111–119 [PubMed: 12383190]
50. Bakowska J, Adamson IY. Collagenase and gelatinase activities in bronchoalveolar lavage fluids during bleomycin-induced lung injury. *J Pathol* 1998;185(03):319–323 [PubMed: 9771487]
51. Schiller HB, Fernandez IE, Burgstaller G, et al. Time- and compartment-resolved proteome profiling of the extracellular niche in lung injury and repair. *Mol Syst Biol* 2015;11(07):819 [PubMed: 26174933]
52. Cleveland ZI, Zhou YM, Akinyi TG, et al. Magnetic resonance imaging of disease progression and resolution in a transgenic mouse model of pulmonary fibrosis. *Am J Physiol Lung Cell Mol Physiol* 2017;312(04):L488–L499 [PubMed: 28130263]

53. Georges PC, Hui JJ, Gombos Z, et al. Increased stiffness of the rat liver precedes matrix deposition: implications for fibrosis. *Am J Physiol Gastrointest Liver Physiol* 2007;293(06):G1147–G1154 [PubMed: 17932231]
54. Hinz B Mechanical aspects of lung fibrosis: a spotlight on the myofibroblast. *Proc Am Thorac Soc* 2012;9(03):137–147 [PubMed: 22802288]
55. Rubin JM, Horowitz JC, Sisson TH, Kim K, Ortiz LA, Hamilton JD. Ultrasound strain measurements for evaluating local pulmonary ventilation. *Ultrasound Med Biol* 2016;42(11):2525–2531 [PubMed: 27520395]
56. Sáez-Royuela F, Linares P, Cervera LA, et al.; Castile and Leon Hepatology Association (ACyLHE). Evaluation of advanced fibrosis measured by transient elastography after hepatitis C virus protease inhibitor-based triple therapy. *Eur J Gastroenterol Hepatol* 2016;28(03):305–312 [PubMed: 26636405]
57. Dillman JR, Stidham RW, Higgins PD, et al. Ultrasound shear wave elastography helps discriminate low-grade from high-grade bowel wall fibrosis in ex vivo human intestinal specimens. *J Ultrasound Med* 2014;33(12):2115–2123 [PubMed: 25425367]
58. Stidham RW, Xu J, Johnson LA, et al. Ultrasound elasticity imaging for detecting intestinal fibrosis and inflammation in rats and humans with Crohn’s disease. *Gastroenterology* 2011;141(03): 819–826 [PubMed: 21784048]



**What is known about this topic?**

- An impairment of plasminogen activation within the lung following injury promotes the development of fibrosis.
- Enhancing plasminogen activation lessens the severity of developing fibrosis in animal models.

**What does this paper add?**

- Upregulating plasminogen activation promotes the resolution of established fibrosis.
- The reversal of established fibrosis is associated with an induction of lung fibroblast apoptosis and a reversal of increased lung stiffness.
- Both early and late upregulation of plasminogen activation following lung injury similarly reduce the severity of fibrosis.

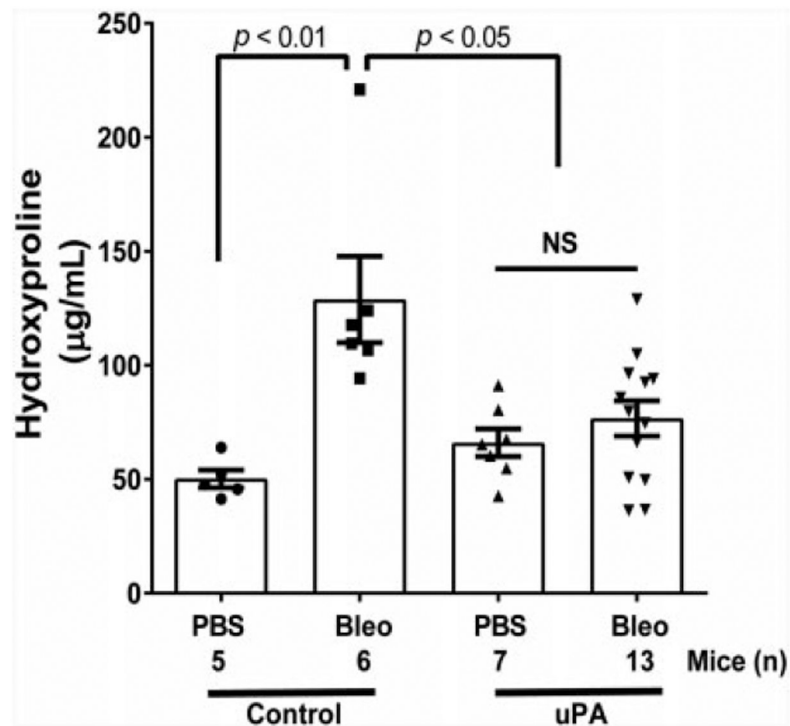


**Fig. 1.** Urokinase plasminogen activator (uPA) overexpression prevents increased lung parenchymal stiffness and lung fibrosis following bleomycin-induced lung injury. uPA double transgenic mice or littermate controls received bleomycin (1.15 U/kg) or phosphate-buffered saline (PBS) via intratracheal administration on day 0. Doxycycline was administered to all mice from day 1 (starting 24 hours after bleomycin administration) through day 28. On day 28, measurements were performed for total lung collagen content via an assay for hydroxyproline. The number of mice assessed in each cohort is shown within the figure.

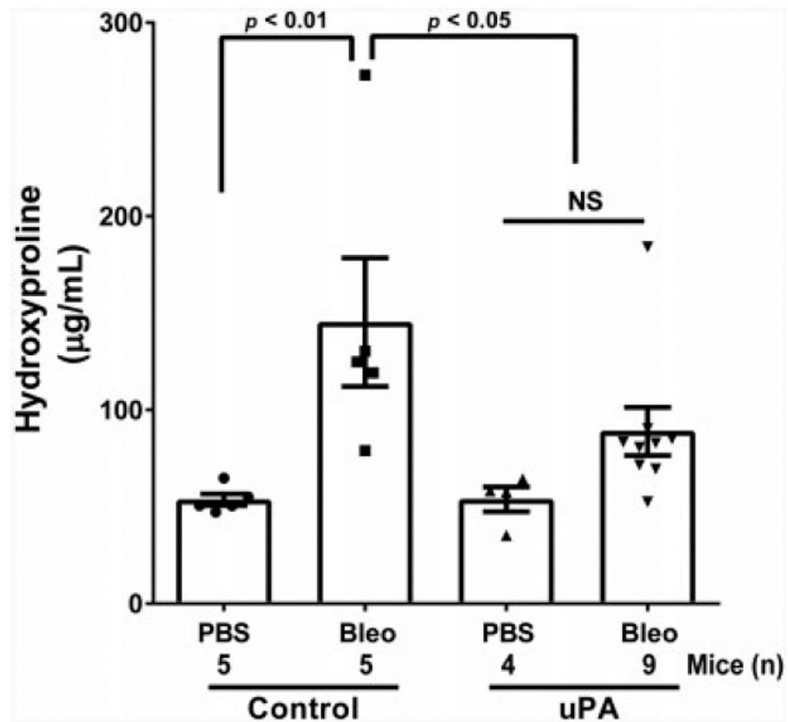


**Fig. 2.**

Postinflammatory urokinase plasminogen activator (uPA) overexpression attenuates increased lung parenchymal stiffness and lung fibrosis following bleomycin-induced lung injury. uPA double transgenic mice or littermate controls received bleomycin (1.15 U/kg) or phosphate-buffered saline (PBS) via intratracheal administration on day 0. Doxycycline was administered to all mice from day 9 through day 28, and lung collagen content was assessed by hydroxyproline quantification. The number of mice included in each cohort is shown within the figure.

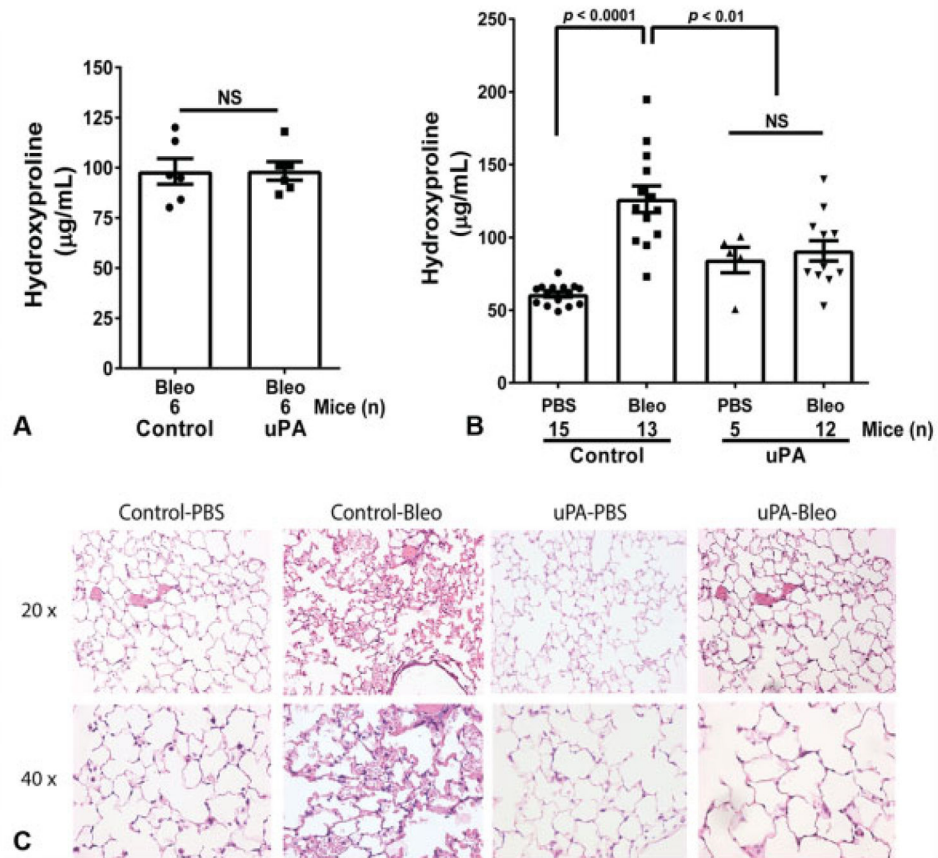


**Fig. 3.** Urokinase plasminogen activator (uPA) overexpression during the fibrotic phase of bleomycin-induced lung injury diminishes fibrosis and reduces parenchymal stiffness. uPA double transgenic mice or littermate controls received bleomycin (1.15 U/kg) or phosphate-buffered saline (PBS) via intratracheal administration on day 0. In a subset of mice (**A**) lung hydroxyproline was quantified at day 14. Doxycycline was then administered to all mice from day 14 through day 28. (**B**) Hydroxyproline was quantified at day 28. (**C**) Lung histology at day 28. The numbers of mice assessed in each cohort and at each time point is shown within the figure.

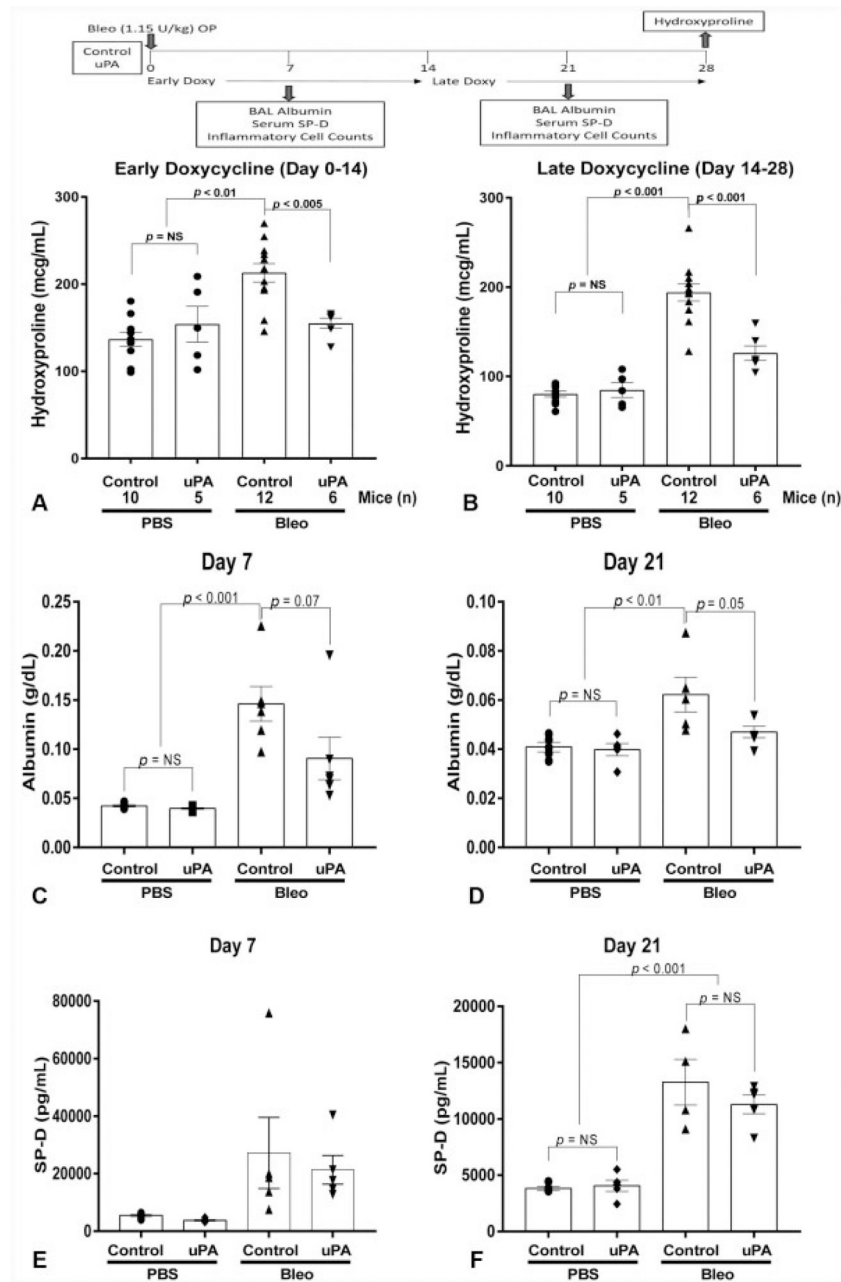


**Fig. 4.** Urokinase plasminogen activator (uPA) overexpression during inflammatory or fibrotic phase of bleomycin-induced lung injury diminishes lung fibrosis: uPA double transgenic mice or littermates (controls) received bleomycin (1.15 U/kg) or phosphate-buffered saline (PBS) via intratracheal administration on day 0. Doxycycline was administered to mice early (days 0–14) and then discontinued (A) or late (days 14–28) (B) and lung hydroxyproline was quantified in both the early and late group at day 28.  $n = 6–12$  mice per cohort. (C, D) Lavage fluid was collected from the lungs after 7 days of doxycycline exposure in both groups: day 7 for early group (C) and day 21 for late group (D) and analyzed for albumin concentration. (E, F) Serum was collected after 7 days of doxycycline exposure for both

groups: at day 7 for early group (**E**) and day 21 for late group (**F**) and analyzed for surfactant protein D (SP-D) concentration. Each figure includes the numbers of mice analyzed within each cohort. Results are displayed as mean  $\pm$  standard error and data was analyzed using one-way analysis of variance (ANOVA).

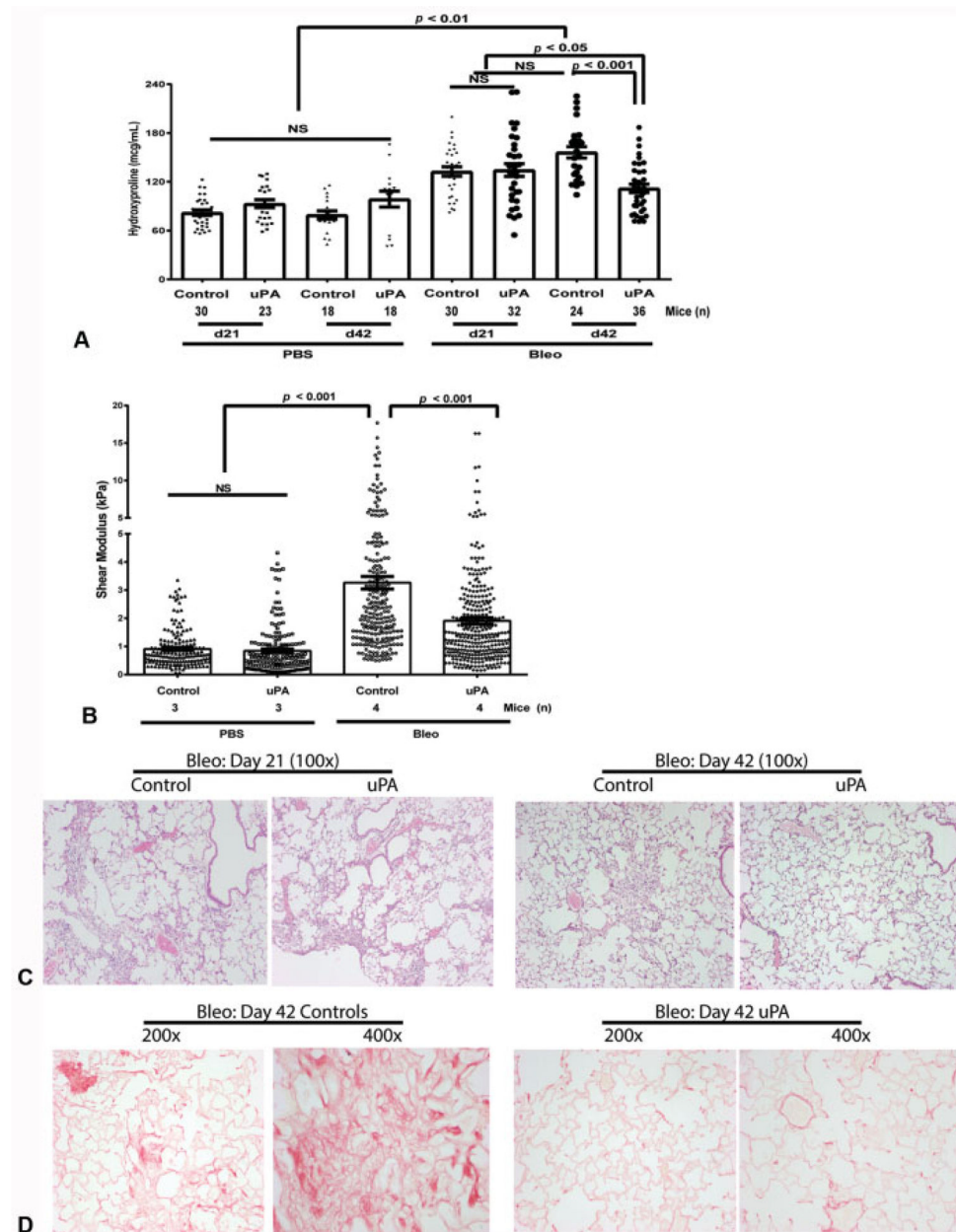


**Fig. 5.** Urokinase plasminogen activator (uPA) overexpression promotes the resolution of established fibrosis and decreases lung parenchymal stiffness. uPA double transgenic mice or littermate controls received bleomycin (1.15 U/kg) or phosphate-buffered saline (PBS) via intratracheal administration on day 0 and doxycycline was administered from days 21 to 42. **(A)** Lung hydroxyproline was assessed at day 21 (prior to doxycycline administration) and day 42 (after 21 days of doxycycline) in control and transgenic mice that received i.t. PBS or bleomycin on day 0. **(B)** Lung stiffness was determined in PBS- and bleomycin-treated control and transgenic mice at day 42 (after 21 days of doxycycline). **(C)** Hematoxylin and eosin staining from bleomycin-treated control and transgenic (uPA overexpressing mice) at day 21 (prior to doxycycline) and day 42 (following 21 days of doxycycline). **(D)** Picrosirius

red staining at day 42 following bleomycin treatment in control and transgenic mice that received doxycycline from days 21 to 42. Representative images are shown at two magnifications. The numbers of mice assessed in each cohort is included within the corresponding figure.

Author Manuscript

Author Manuscript

Author Manuscript

Author Manuscript



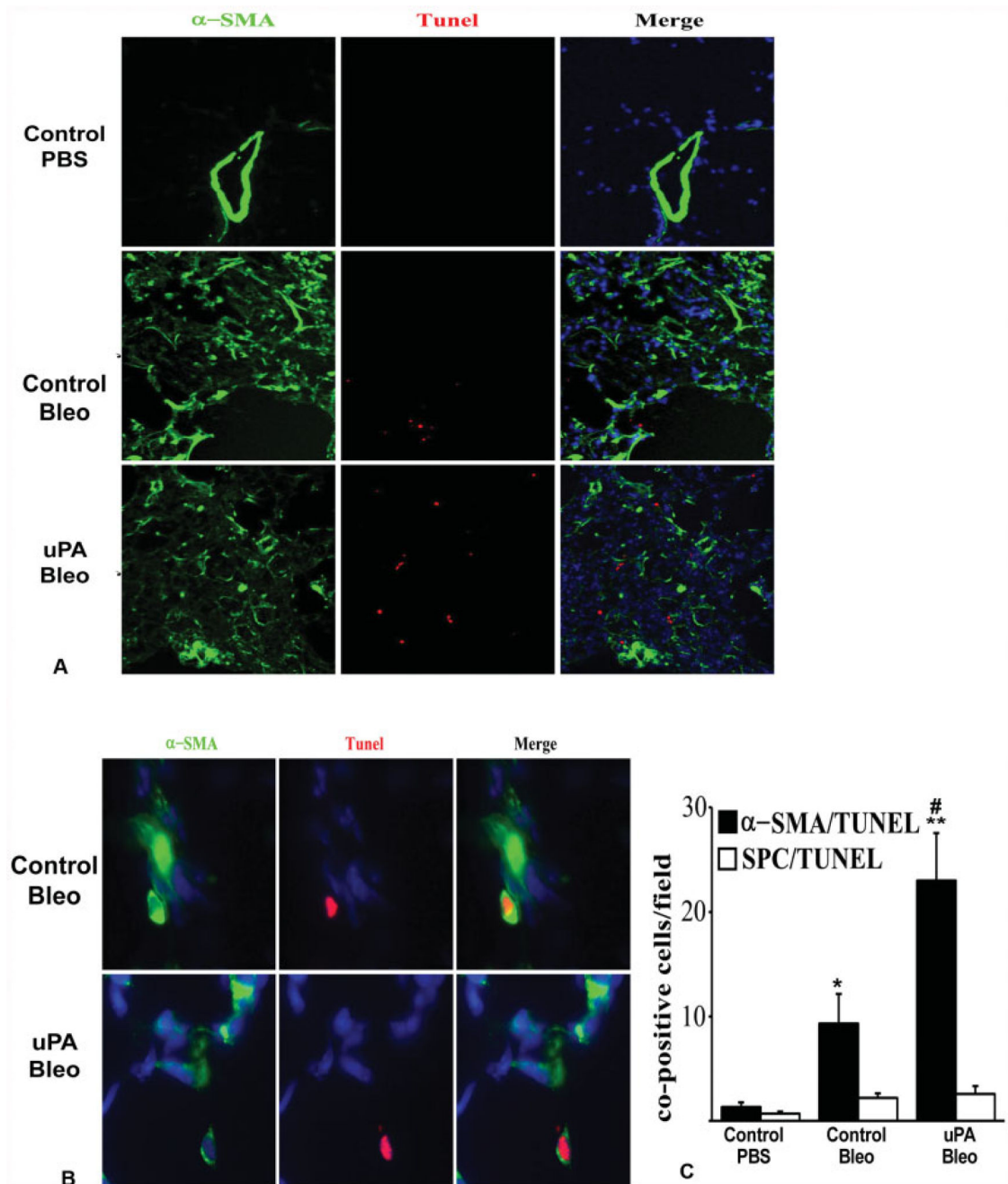


**Fig. 6.** Urokinase plasminogen activator (uPA) overexpression enhances myofibroblast apoptosis: uPA overexpressing double transgenic mice or littermate controls received bleomycin (1.15 U/kg) via intratracheal administration on day 0. Doxycycline was administered from days 21 to 24, at which time lungs were fixed and myofibroblast apoptosis was assessed by (A) costaining for terminal deoxynucleotidyl transferase dUTP nick end labeling (TUNEL) (red) and  $\alpha$ -smooth muscle actin (green). Nuclei were identified by 4',6-diamidino-2-phenylindole (DAPI) staining (blue). Images were taken at 40 $\times$ . (B) Representative high-power (100 $\times$ ) images from lung tissue costained with  $\alpha$ -smooth muscle antibody (SMA)

and TUNEL demonstrates  $\alpha$ -SMA with a cytoplasmic distribution and accumulation of TUNEL stain with a nuclear distribution as indicated by colocalization with DAPI. (C) Myofibroblast and type 2 alveolar epithelial cell apoptosis were assessed by an investigator who was blinded to the genetic background and treatment cohorts who counted the number of  $\alpha$ -SMA or surfactant protein C (SPC) positive cells that costained with TUNEL. Representative images from SPC and TUNEL double-positive cells are shown in ►Supplementary Fig. S1.  $*p < 0.05$  and  $**p < 0.001$  compared with control/phosphate-buffered saline (PBS).  $\#p < 0.01$  compared with control/bleomycin. There was no statistically significant differences between cohorts in SPC/TUNEL costained cells.